The interplay of wind and uplift facilitates over-water flight in facultative soaring birds

Elham Nourani [*1,2], Gil Bohrer [3], Paolo Becciu[1,2,4], Richard O. Bierregaard[5], Olivier Duriez[6], Jordi Figuerola[7], Laura Gangoso[8,9,7], Sinos Giokas[10], Hiroyoshi Higuchi[11], Christina Kassara[10], Olga Kulikova[2,12], Nicolas Lecomte[13], Flavio Monti[14], Ivan Pokrovsky[1,12,15], Andrea Sforzi[16], Jean-François Therrien[17], Nikos Tsiopelas[18], Wouter M.G. Vansteelant[7,9], Duarte S. Viana[19,20], Noriyuki M. Yamaguchi[21,22], Martin Wikelski[1,2,23], and Kamran Safi[1,2].

[1] Department of Migration, Max Planck Institute of Animal Behavior, Germany.

[2] Department of Biology, University of Konstanz, Germany.

[3] Department of Civil, Environmental and Geodetic Engineering, The Ohio State University, United States of America.

[4] Department of Evolutionary and Environmental Biology, and Institute of Evolution, University of Haifa, Israel.

[5] Ornithology Department, The Academy of Natural Sciences of Drexel University, United States of America.

[6] Centre for Evolutionary and Functional Ecology, Montpellier University-CNRS, France.

[7] Department of Wetland Ecology, Estación Biológica de Doñana, Spain.

[8] Department of Biodiversity, Ecology and Evolution, Faculty of Biology, Complutense University of Madrid, Spain.

[9] Institute for Biodiversity and Ecosystem Dynamics (IBED), University of Amsterdam, The Netherlands.

[10] Department of Biology, University of Patras, Greece.

[11] Research and Education Centre for Natural Sciences, Keio University, Japan.

[12] Institute of the Biological Problems of the North, Russian Academy of Sciences, Russia.

[13] Canada Research Chair in Polar and Boreal Ecology, Department of Biology, University of Moncton, Canada.

[14] Department of Physical Sciences, Earth and Environment, University of Siena, Italy.

[15] Institute of Plant and Animal Ecology, Russian Academy of Sciences, Russia.

[16] Maremma Natural History Museum, Italy.

[17] Hawk Mountain Sanctuary, Acopian Center for Conservation Learning, United States of America.

[18] Hellenic Ornithological Society/BirdLife Greece, Greece.

[19] German Center for Integrative Biodiversity Research (iDiv) Halle-Jena-Leipzig, Germany.

[20] Leipzig University, Germany.

[21] Graduate School of Fisheries and Environmental Sciences, Nagasaki University, Japan.

[22] Organization for Marine Science and Technology, Nagasaki University, Japan.

[23] Centre for the Advanced Study of Collective Behaviour, University of Konstanz, Germany.

[*] **Corresponding author:** enourani@ab.mpg.de, mahle68@gmail.com

Abstract

Flying over the open sea is energetically costly for terrestrial birds. Despite this, over-water journeys of many terrestrial birds, sometimes hundreds of kilometers long, are uncovered by bio-logging technology. To understand how these birds afford their flights over the open sea, we investigated the role of atmospheric conditions, in the form of wind and uplift, in subsidizing over-water flight at the global scale. We first established that ΔT, the temperature difference between sea surface and air, is a meaningful proxy for uplift over the open sea. Using this proxy, we showed that the spatio-temporal patterns of sea-crossing in terrestrial migratory birds is associated with favorable uplift conditions. We then analyzed route selection over the open sea for four facultative soaring species, representing all major migratory flyways worldwide. Our results showed that favorable uplift conditions, albeit not as common and powerful as over land, are not rare over the open sea. As expected, birds maximized wind support when selecting their sea-crossing routes, but also selected higher uplift when suitable wind support is available. Our findings suggest that uplift may play a key role in the energy seascape for bird migration that in turn determines strategies and associated costs for birds crossing ecological barriers such as the open sea.

Keywords: Energy landscape, migration, soaring, bio-logging, route selection, movement ecology.

Introduction

Dynamic atmospheric conditions largely define the energetic costs of flight for birds. Tail winds, for example, permit birds to reduce air speed while maintaining the speed of travel, helping them to save energy [1, 2]. Likewise, rising air as a consequence of warm air columns known as thermals and orographic uplift created by the interplay between wind and topography, can push flying animals upwards and reduce the energetic costs of remaining airborne [3–5]. However, the energy availability landscape [6] is interspersed with patches where energetic subsidies in the atmosphere are weak or absent, impeding efficient movement. Flight over such areas becomes energetically costly, yet some animals regularly engage in such seemingly risky flights, particularly during migration [7, 8]. How birds afford their flights across such migratory barriers remains an open and important question for understanding the evolution of migratory routes and sea-crossing strategies.

The open sea is considered a major migratory barrier for all terrestrial species, and particularly for soaring birds [8, 9]. This is rooted in observational studies of birds gathering in large numbers at bottlenecks prior to setting out over even relatively short over-water passages [8, 10]. The existence of such large aggregations, together with the technological difficulty of observing birds over the open sea, led to a general understanding that sea-crossing poses a formidable challenge for birds that are unable to land or forage at sea [11]. Yet, some early studies looked beyond the role of geography alone and suggested that the extent to which terrestrial birds aggregate through overland flyways vary greatly across space and time [12–14]. They further suggested that weather plays an important role in terrestrial birds' ability to embark on, and sustain, over-water flight [15]. Advances in bio-logging technology have since created clearer picture of sea-crossing behavior in terrestrial birds.

Bio-logging has confirmed extremely long sea-crossings in terrestrial birds [16, 17]. It has provided evidence that the prevalence and extent of this behavior varies in different migratory flyways [8, 11] and seasons [18, 19], as well as based on morphological characteristics [20]. We now have ample evidence that, in most cases of sea-crossings, atmospheric support, mostly in the form of wind support (i.e. the length of the wind vector in a bird's flight direction) is an important facilitator [18, 21–24].

An emerging hypothesis is that uplift also plays a role in the energy seascape for soaring bird migration. Uplift can reduce the energetic costs of remaining airborne. Additionally, soaring birds could take advantage of strong uplift to soar. Past bio-logging studies measured flight altitude in soaring birds to provide indirect proof of thermal soaring behavior at sea [25, 26]. More recently, high resolution GPS tracking documented the circling flight pattern and vertical aerial climb of migrating ospreys over the Mediterranean Sea [27]. This study also confirmed the earlier suggestions that ΔT, defined as the difference in temperature between the sea surface and the air, can be used as a proxy for uplift potential over water [28]. Positive ΔT values correspond to upward moving air, while negative values can be interpreted as sinking air, termed subsidence. This proxy was consequently adopted to quantify the energy seascapes that enable juvenile European honey buzzards to survive longer sea-crossings compared to their earlier migrating adult conspecifics [19]. Yet, whether ΔT is a meaningful correlate of upward moving air has not been quantitatively tested.

In this study, we investigate sea-crossing behavior at the global scale to assess the role of uplift and wind in shaping the energy seascapes for terrestrial bird migration. To do this, we use bio-logging data collected for five raptor species that perform long sea-crossing journeys. These species differ in size, morphology, and stop-over strategies, and their overall dependence on soaring flight to cover long distances. However, they are all facultative soaring migrants and might be expected to preferentially use soaring over flapping flight whenever possible, including flights over open water. This provides an opportunity to investigate sea-crossing behavior at all major migratory flyways at spatio-temporal scales equivalent to that of the publicly available global atmospheric information. Using these data, we set out to establish whether ΔT is a meaningful proxy for uplift potential over water, by testing its correlation with convective velocity (w^*; [29]). We further hypothesize that (i) sea-crossings are associated with temperature gradients that are indicative of uplift in all flyways and (ii) both wind and ΔT influence over-water route selection.

Methods

Bio-logging data set

We compiled a bio-logging data set containing migratory trajectories of birds that regularly perform sea-crossings during autumn. We did not include spring migration in this study, due to the limited amount of data for spring migration compared to autumn. Our data set was comprised of five species: the Oriental honey buzzard *Pernis ptilorhynchus* and the grey-faced buzzard *Butastur indicus* in the East Asian flyways, the osprey *Pandion haliaetus* and the peregrine falcon *Falco peregrinus*, in both the African-Eurasian and the American flyways, and the Eleonora's falcon *F. eleonorae* in the African-Eurasian flyway. These birds are all facultative soaring birds. Their dependence on uplift varies, with the falcons and the osprey being less dependent on uplift than the buzzards [11].

We focused only on sea-crossing behavior during migration to ensure a common flight purpose among all species and individuals in the analyses. We only included adults as they actively select their route based on experience, unlike juveniles that follow an innate direction of migration, likely without established route selection criteria (e.g.[30, 31]). We limited our analysis to sea-crossing trips longer than 30 km, which corresponded to the spatial resolution of our environmental data (see Route selection analysis below).

Correlation of $\triangle T$ and convective velocity

To determine whether $\triangle T$ is a meaningful measure of uplift velocity, we calculated the correlation between this variable and the convective velocity scale, *w** [29]. *w** is estimated on the basis that the buoyancy associated with surface heat flux produces uplift:

$$w^* = [gz(\frac{(w'T') + 0.61T_{2m}(w'q')}{\theta})]^{\frac{1}{3}}$$

where *g* [m/s^2] is the gravitational acceleration, *z* [m above reference sea level] is the depth of the atmospheric boundary layer, the term *(w'T'+0.61* T_{2m}*(w'q'))* approximates the surface virtual potential temperature flux, where *(w'T')* [K m/s] is the surface temperature flux and *(w'q')* [g_{water}/kg_{air} m/s] is the surface water vapor flux and T_{2m} [C] is the air temperature near the sea surface. θ [K] is the virtual potential temperature at the height of the boundary layer top (*z*), and was approximated using the wet adiabatic lapse rate (typical for oceanic boundary layers) as

$$\theta = T_{2m} + 273.15 + 0.006z$$

We used data from the ERA-interim reanalysis database (Spatial and temporal resolution of 0.75 degrees and 3 hours, respectively) provided by the European Center for Medium-Range Weather Forecast (ECMWF; *https://www.ecmwf.int*). We accessed these data through the EnvDATA service [32] on Movebank (*www.movebank.org*), to get the values for *z*, T_{2m}, *w'T'* and *w'q'* (with some unit conversions). Overall, we closely followed Bohrer et al. [33] to calculate *w**, but including the contribution of the surface water vapor flux to the surface virtual potential temperature flux, and using the wet adiabatic laps rate to estimate the potential temperature at the height of the boundary layer top.

*w** represents uplift and can only be calculated for positive heat fluxes. Hence, we calculated *w** for all the sea-crossing points in our bio-logging data set where $\triangle T$ was positive and estimated the correlation (Pearson's product-moment correlation coefficient) between the two variables.

Spatio-temporal modeling of $\triangle T$

To show the spatio-temporal variation in $\triangle T$ at the global scale, we used 40 years of temperature data. We focused on five regions, where regular long-distance sea-crossing is performed by facultative soaring birds, namely South-East Asia, the Indian Ocean, the Mozambique Channel, Europe, and the Americas. We downloaded sea-surface temperature and temperature at 2 meters above the sea for these regions for 1981-2020 from the ECMWF ERA-interim reanalysis data set (Spatial and temporal resolution of 6 hours and 0.75°,

respectively). We chose to use this data set instead of the higher resolution ERA5, to reduce the time and memory needed for carrying out the analysis. We spatially filtered the data to exclude lakes, as we were only interested in the open seas and oceans. To include a proxy for the time of day, we calculated the solar elevation angle for each data point. We then created a categorical variable with three levels, night, low sun elevation, and high sun elevation, corresponding to sun elevation angles below -6, between -6 and 40 degrees, and over 40 degrees, respectively.

We loosely followed Nourani et al. [19] to construct energy seascapes. In brief, we modeled ΔT as a function of latitude, longitude, day of year, and time of day using the generalized additive mixed modeling (GAMM) approach. Five models were constructed in total, one per region. We extracted the timing and location of sea-crossings from our bio-logging data set. We did not have empirical data for bird migration over the Indian Ocean and therefore consulted the relevant literature to extract the spatio-temporal pattern of the Amur falcon's *Falco amurensis* sea-crossing over the region [34, 35]. Each model included two smoothers, one cyclic cubic regression splines smoother for the day of the year and a spline on the sphere for latitude and longitude. For both of these parameters, one smoothing curve was estimated for each level of time of day. Year was added as a random intercept in the models to control for annual variations in ΔT. We also included a variance structure in the models to account for the heteroscedasticity caused by higher ΔT variance in higher latitudes. Models were fitted using the mgcv package [36] in R ver. 4.0.2 [37].

We used each model to predict energy seascape maps for the autumn migration season (August-November). We spatially interpolated the prediction rasters to a 1 km resolution, for visualization purposes.

Route selection analysis

We investigated route selection by fitting a step selection function [38] to relate the probability of presence over the sea with atmospheric conditions. Every two consecutive points along a track were considered a step. Atmospheric conditions were compared between the observed step and a set of alternative steps that were available to the birds in space and time. The grey-faced buzzard was excluded from this analysis because of the low resolution of the satellite-tracking data.

We filtered our data set to include only points over the open sea. Trajectories that intersected land, e.g. islands, were broken into sea-crossing segments. Segments shorter than 30 km, and those that included fewer than 3 tracking points, were removed. To ensure a uniform temporal resolution and to reduce spatio-temporal auto-correlation, we re-sampled all data to one-hourly intervals (with a tolerance of 30 minutes; see thinTrackTime in package Move [39]). In the resulting data set, we had 19 and 25 individuals for Eleonora's falcons tracked from Spain and ospreys tracked in the Americas, respectively. All other groups were represented by less than 10 individuals. To ensure a more even representation of different groups in the final data set, we randomly selected 10 individuals form the two over represented groups (Electronic supplementary material Table S1).

We prepared a stratified data set for analysis: along each sea-crossing segment, for each step, we generated 50 spatially alternative steps based on the distribution of step lengths (Gamma distribution) and turning angles (von Mises distribution) of the empirical data, so that each stratum had 1 used and 49 alternative steps.

All data were then annotated using the ENV-data track annotation service [32] provided by Movebank. Each point was annotated with u (eastward) and v (northward) components of the wind, sea-surface temperature, and temperature at 2 m above the sea, all provided by ECMWF ERA5 reanalysis database (temporal and spatial resolution of 1 hour and 0.25°, respectively). We selected the bilinear and the nearest-neighbour methods of interpolation for the wind and temperature data, respectively. We then calculated wind support [40], wind speed, and ΔT using the annotated data. Additionally, to investigate whether predictability of atmospheric conditions affected the sea-crossing route choice, we annotated each point with long-term variances (over 40 years; 1981-2020) for wind support and ΔT.

We checked the annotated data set for multicollinearity and only considered variables that were not highly correlated ($r < 0.6$). Prior to analysis, we converted all values of explanatory variables to z-scores (i.e. the distance of a raw value from the mean, measured in units of standard deviation) to ensure comparability among predictors.

Step selection functions were then estimated using the Integrated Nested Laplace Approximation (INLA) method using the INLA package [41] in R ver. 4.0.2 [37]. Model fitting procedure and priors were based on Muff et al. [42]. We constructed a multilevel model with fixed effects for ΔT, wind support, wind speed, long-term variance wind support, as well as an interaction term for wind support and ΔT. Species and individual IDs (nested within species) were included as random effects on the slopes. To construct alternative models, in a step-wise manner, we removed explanatory variables with non-significant coefficients (i.e. with credible intervals including zero). We then compared the alternative models using conditional predictive ordinates (CPO), a cross-validation criterion for model assessment, and log of marginal likelihood (MLik), which shows the probability of the observed data under a given model ([43]). The model with the lowest CPO and MLik scores was considered the best.

Results

We found a positive correlation between the convective velocity scale, w^*, and ΔT ($r = 0.49$; $p < 0.05$). The sea-crossing data from all species showed overnight flights (Fig.1, Electronic supplementary material Fig. S4). There was no clear difference between the pattern of correlation between w^* and ΔT in different times of the day or for different species (Fig.1).

The spatio-temporal pattern of sea-crossing in the six terrestrial bird species (the five species in our biologging data set, plus Amur falcon) corresponded with positive uplift potential over the open sea (Fig. 2; see subplots for within-year and within-day variations in each region; see electronic supplementary material Table S2 for detailed GAMM outputs). The osprey was the only species flying over the open sea when the sea surface was colder than the air (i.e. negative ΔT). This pattern occurred over both the Mediterranean and the Caribbean Seas (Fig. 2). The Eleonora's falcons flying over the Mozambique Channel also experienced relatively low and sometimes negative ΔT (Electronic supplementary material Fig. S4). However, over-water flight in the absence of uplift did not set the two species apart from the other species in route selection criteria. We did not find significant species-specific differences in route selection in our step selection analysis (Electronic supplementary material Fig. S1).

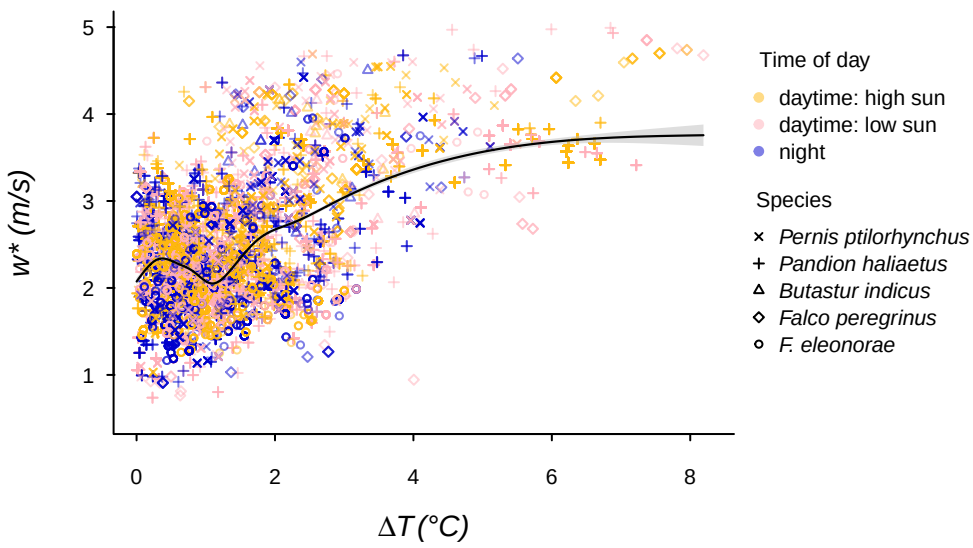

Figure 1: Relationship between ΔT and the convective velocity, w^* (for all points with positive ΔT). The sea-crossing bio-logging data (pooled for all five species) were annotated with values of ΔT and w^*. The smooth curve shows cubic regression splines fitted to the data (r^2 *(adj.)* = 0.31; $p < 0.05$) predicting w^* as a function of ΔT (with the 95% confidence interval). Colors and shapes represent different times of day and species, respectively.

We analyzed over-water route selection in 66 sea-crossing tracks of 42 individuals (Electronic supplementary material Table S1 and Fig. S3). We did not include the long-term variance of ΔT in the model, as it was correlated with the instantaneous ΔT values ($r = 0.63$; $p < 0.05$). The most important variable determining over-water route selection was wind support, with a positive effect. The interaction between ΔT and wind support also showed a positive, yet smaller, effect (Fig. 3). ΔT had a negative impact on route selection. Wind speed was not significant and was dropped from the models. Model 3 performed best in terms of both CPO and MLik (Table 1).

Discussion

We found that, at the global scale, facultative soaring birds were more selective for wind support than uplift when flying over the open sea. This confirms previous findings that birds aim at maximizing wind support, probably to reduce the time and energy required to complete their journeys. [18, 21–24, 44–46]. Our models

Table 1: Model specifications for the step selection function analysis using INLA. Fixed effects included ΔT, wind speed (wspd), wind support (wspt) and long-term variance of wind support (wspt var).The model with the lowest CPO and MLik values (Model 3) was selected as the best model.

Model	Fixed effects	Random effects	CPO	MLik
1	ΔT * wspt + wspd + wspt var	species, ID	80446.77	-13499.52
2	ΔT * wspt + wspt var	species, ID	76024.6	-13513.37
3	ΔT * wspt	species, ID	74560.95	-13640.09

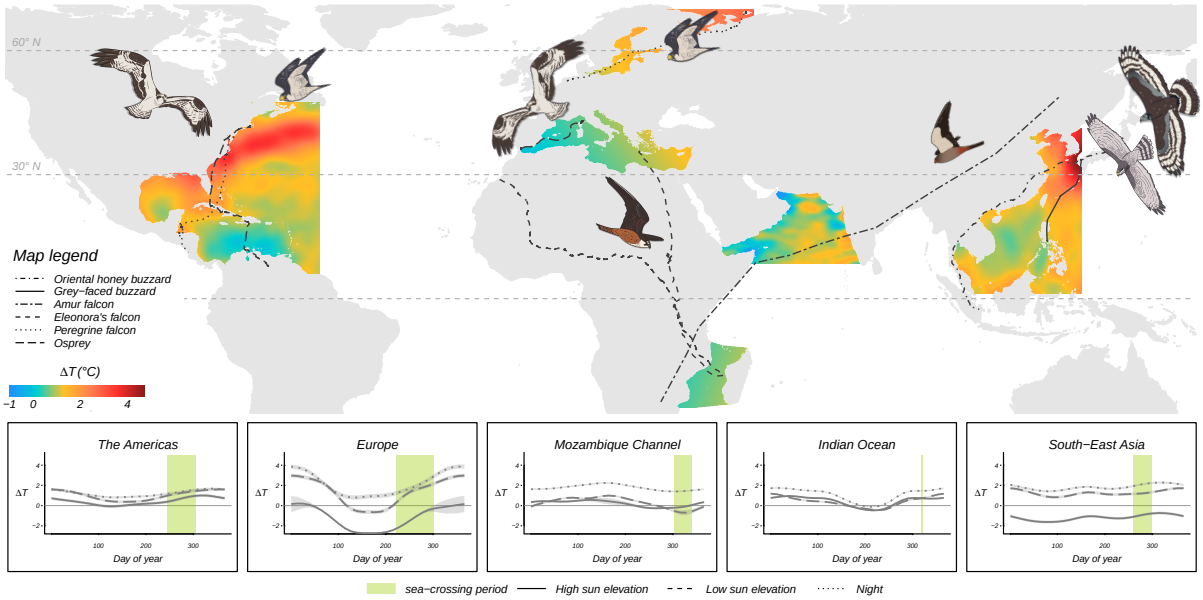

Figure 2: Energy seascapes for soaring bird migration in autumn. The map shows the energy seascapes for August-November derived from 40 years of temperature data. Tracks correspond to sample migratory trajectories. All tracks are based on empirical data, except for the Amur falcon, which is based on the available literature [35]. Subplots show the distribution of ΔT throughout the year in each region, for each time of day (based on summed effects from the GAMMs with 95% confidence intervals). Green shaded areas in the subplots show the timing of sea-crossing in the species flying over the corresponding region.

also showed a positive effect of the interaction between wind support and ΔT. This indicates that when wind support is favorable, the birds also select high values of ΔT to gain better advantage of uplift.

Contrary to our expectations, after accounting for the other variables, higher ΔT values alone had a lower probability of being chosen on route selection. This suggests that in the absence of suitable wind support, the birds did not choose stronger uplifts to fuel their flights. Still, we do show that uplift conditions over the sea were generally favorable during the birds' autumn migration season (Fig. 2) as well as at the start of sea-crossing (Electronic supplementary material Fig. S4). We speculate that the birds may avoid turbulent conditions by avoiding high ΔT. The fact that the birds mostly encountered positive ΔT along their over-water routes (Electronic supplementary material Fig. S2 and S3) indicates that even when selecting low values of ΔT, they still were very likely to experience some amount of uplift regardless, and would not prefer higher uplift for forgoing better wind support.

The sea surface tends to be warmer than the air in autumn, creating upward heat flux. This is reflected in our global energy seascape map (Fig. 2). The mostly positive values of ΔT on this map indicates that the spatio-temporal patterns of sea-crossing in autumn is associated with favorable uplift conditions, supporting our first hypothesis. Moreover, the range and mean of ΔT values were similar between the observed and alternative steps in our step selection function estimation (Electronic supplementary material Fig. S2). The birds thus faced more variability in wind conditions than in uplift, which can further explain why wind support

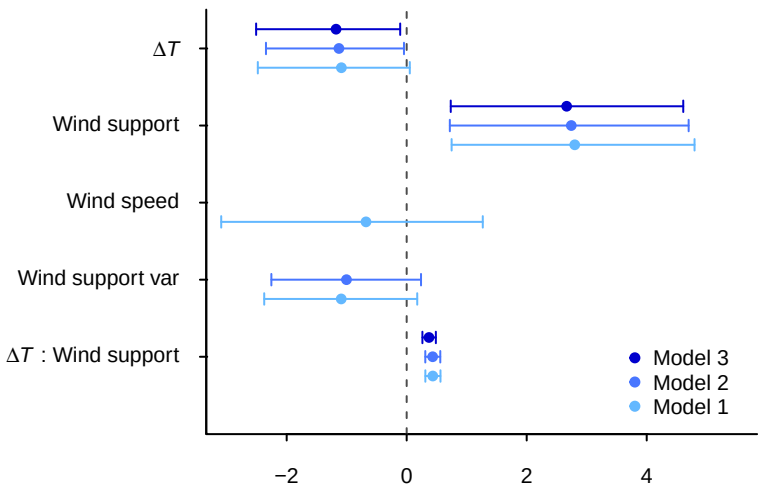

Figure 3: Posterior means (z-scores) and 95 % credible intervals for the fixed effects in the INLA models. Model names correspond to those in Table 1.

was the most important criterion for route selection (Table 1). We further showed that ΔT has a relatively low seasonal variation, except in Europe (subplots in Fig. 2). As a result, birds flying along these flyways in spring could potentially benefit from uplift. However, we cannot make generalizations about sea-crossing patterns in spring based on ΔT alone. As our route selection analysis showed, wind support plays a more important role in over-water flight than uplift. Even in similar uplift conditions between the two seasons, variations in wind support can lead to loop migration patterns [47, 48] and even avoidance of sea-crossing in one season [18]. Uncovering the role of atmospheric subsidies in shaping sea-crossing patterns in spring requires multi-species bio-logging data, which were not available to our study.

Evidence for soaring flight over the sea has accumulated for at least a decade. Yet, many studies overlook uplift potential when explaining sea-crossing behavior. This could be due to the presumption that thermals do not form over the sea, as well as a lack of a reliable and easy to compute proxy for uplift over water. Studies that try to investigate uplift do so by using a variety of proxies, including air temperature [49], air temperature gradient [18], vertical air velocity [18], boundary layer height [50], and solar irradiance [51], which makes interpretation of the results and comparisons among studies difficult. ΔT is shown, by direct observations [52] and bio-logging technology [27], to be related to soaring flight. Our results confirming the correlation of ΔT with w^*, a widely accepted measure of uplift by the movement ecology community (so far mostly used to estimate uplift over land [33]), further point to the potential of this proxy as a measure of uplift over the open sea. Duriez et al. [27] showed that ospreys predictably engaged in thermal soaring over the Mediterranean Sea when ΔT values were higher than 3°C. Although we provide a range of w^* values (m/s) for each value of ΔT in our data, the resolution of our data did not allow us to directly investigate whether and in what ΔT conditions the birds engaged in soaring flight. In fact, there remains a strong need for quantifying the amount of energy, or the realized uplift, that a bird can gain from ΔT. Theoretical and high-resolution multi-sensor bio-logging studies can investigate this for birds with different morphological characteristics and under different wind conditions.

Although we show that it is possible to estimate w^* using publicly available weather data, it is not an ideal proxy for measuring uplift under all circumstances over the open sea. Firstly, w^* can only be estimated for

upward moving air. This means that there will be no values estimated for subsidence. ΔT does not have this limit, as it provides positive values for uplift and negative values for subsidence. Secondly, calculating w^* requires at least a basic knowledge of meteorological concepts and units. Different reanalysis data sets provide different variables for potential and water vapor fluxes, making our method of calculating w^* difficult to adapt for other studies. This is while ΔT can be calculated only using two simple variables, sea-surface and air temperature, and yields the same result whether temperature data is obtained in units of Kelvin or Celsius. It is therefore a more approachable and possibly reliable measure than w^*. Lastly, although it is ideal to be able to calculate uplift in meters per second, w^* has not been ground-truthed. We cannot be sure whether our estimated w^* values are a precise representation of the strength of uplift over water. Although ΔT does not provide realized uplift, it is an intuitively interpretable measure of uplift potential.

Uplift reduces the energetic costs of remaining airborne, for both soaring and flapping flyers. We used facultative soaring species as our model system. These species varied in morphological characteristics and soaring flight dependencies. Yet, we found no significant species-specific variation in the impact of wind support and uplift on their sea-crossing behavior (Electronic supplementary material Fig. S1). This indicates that the patterns that we found can be true for sea-crossing in other species as well. Moreover, our study included all major bird migration flyways. As a result, our findings can further shed light on the energy seascapes other animals flying over these flyways would encounter. For example, the relatively high uplift during the night compared to daytime (Fig. 2) means less drag and could lead to energetically cheaper flight in nocturnal migrants over the Mediterranean [53, 54] and the Caribbean [55, 56] Seas (but see [57] for a suggestion that songbirds prefer non-turbulent air for sea-crossing). Moreover, dragonflies [58] and cuckoos (*Cuculus* spp.; [59]) migrate within the same time window as the Amur falcon over the Indian Ocean (Fig. 2), perhaps taking advantage of the energetic subsidy that the atmosphere provides.

Conclusion

The literature on migratory behavior is increasingly recognizing that atmospheric conditions can reduce the risks associated with sea-crossing in terrestrial birds. Evidence of the role of wind support as a facilitator of this behavior for many species is mounting. Yet, not much is known about the role of uplift. Our findings confirm the role of wind support as the main facilitator of over-water flight, but also provide evidence for widespread uplift potential over the open sea, at least in autumn. We provide quantitative evidence that ΔT is a meaningful proxy for uplift over the open sea. We encourage future studies to take advantage of this proxy, not least because widespread use of ΔT will make comparisons among studies possible. Our findings suggest that the energetic costs of sea-crossing for soaring birds could be at least partially alleviated by overseas uplift. This may have important consequences for shaping routes, timing, and strategies of birds crossing ecological barriers.

Ethics

Capture and tagging of ospreys in Europe were authorized by Istituto Nazionale per la Protezione e la Ricerca Ambientale (ISPRA) and the National authority in Italy for Environmental Research and Protection. The Ministry of Environment and Energy (Greece) granted permission for capturing and tagging Eleonora's falcons (License numbers: 6XΨA0-OKT, Ψ9Θ24653Π8-PT3). The capture and tagging of Eleonora's falcons from

Spain were authorized by the Regional Government of the Canary Islands (Permit numbers: ES-000844/2012, ES-000642/2013, 2014/2224, 2015/3835, 2017/6829). Oriental honey buzzards were tracked under permits no.1705311 (Ministry of the Environment, Japan) and no.6 (Aomori Prefecture). Capture and tagging of ospreys in North America were authorized by the USGS permit no. 20096 (USA) and scientific collecting permit 10907 (Canada). The work was approved by the University of North Carolina at Charlotte's IACUC, protocol 08-024, and by the IACUC of Drexel University, protocol 20632. The peregrine falcons in North America were captured under USGS permit no. 22749 and the state of New Jersey no. SC 2016120. Work on Peregrine falcons in Russian was done under permit No. 77-18/0854/4388 from The General Radio Frequency Centre, permit No. RU/2018/406 from Federal Service for Supervision of Communications, Information Technology and Mass Media (Roskomnadzor), and permit No. RU0000045099 from Federal Security Service. No specific permissions were required from Federal Service for Supervision of Natural Resources (Rosprirodnadzor) according to §44 and §6 of the Federal Law of the Russian Federation No. 52 from 24.04.1995 (last update 24.04.2020) "On Wildlife", and from Federal Service for Technical and Export Control (FSTEC/FSTEK) according to Russian Federation government decree No. 633 from 29.08.2001 and Letter from FSTEK No. 240/33/1373 from 06.04.2015.

Data accessibility

All tracking data used in the route-selection analysis is available as a supplementary material. R codes are available at *https://github.com/mahle68/global_seascape_public*.

Authors' contributions

EN conceived the study and designed the analyses with input from KS and PB. EN conducted the analyses and wrote the paper. GB provided guidance for estimation of w^*. ROB, OD, JF, LG, SG, HH, CK, OK, NL, FM, IP, AS, JFT, NT, WMGV, DSV, NMY, and MW contributed data. All authors commented on and edited the manuscript drafts.

Competing interests

We declare we have no competing interests.

Funding

Tagging and tracking of Eleonora's falcons from Greece were conducted in the framework of the project "LIFE13 NAT/GR/000909 Conservation measures to assist the adaptation of *Falco eleonorae* to climate change" with the financial support of the European Union LIFE Instrument and the Green Fund. Tracking of Eleonora's falcons from Spain was partly funded by the Cabildo de Lanzarote, European Social Fund, and adaptation and improvement of the internationalization of e-infrastructure of the ICTS-RBD for the ESFRI-LifeWatch. UvA-BiTS studies are facilitated by infrastructures for e-Ecology, developed with the support of LifeWatch, and conducted on the Dutch national e-infrastructure with the support of SURF Cooperative. Oriental honey

buzzards were tracked as part of a project commissioned by the New Energy and Industrial Technology Development Organization (NEDO) in Japan. Tracking of ospreys in the Mediterranean was financially supported by the Foundation Prince Albert II de Monaco and the Associazone Italiana della Fondation Prince Albert II de Monaco ONLUS, the Corsica Natural Regional Park (France), the Maremma Regional Park Agency (Italy) and the Tuscan Archipelago National Park (Italy). PB was financially supported by Erasmus+ ICM programme of the European Union and the University of Haifa.

Acknowledgements

We thank all the people and institutions that supported fieldwork and data collection: A. Evangelidis, T. Fransson, T. Curk, P. Glazov, T. Nakahara, F. Nakayama, T. Suzumegano, D. Jennings, R. Julian, I. MacLeod, G. Hickey, J.J. Moreno, W. Bouten, M. de la Riva, J.L. Barroso, M. Majem, the "Progetto Falco pescatore" team, the protected areas of Maremma Regional Park, Tuscan Archipelago National Park, Diaccia Botrona Nature Reserve, WWF Orbetello Lagoon and Orti-Bottagone Nature Reserve in Italy, Massachusetts Audubon, Delaware State Parks, Newfoundland Power, Eversource Energy, the Jane B. Cook 1983 Charitable Trust, 3M, Squam Lakes Natural Science Center's Innovative Project Fund, and Meredith Bay Colony Club in USA, and the Canada Research Chair Program. We would like to thank Damien Farine, Michael Chimento, and Emily Shepard for their comments on the manuscript.

References

1. Liechti, F., 2006 Birds: blowin'by the wind? *Journal of Ornithology* **147**, 202–211. (doi:10.1007/s10336-006-0061-9).

2. Amélineau, F., Péron, C., Lescroël, A., Authier, M., Provost, P. & Grémillet, D., 2014 Windscape and tortuosity shape the flight costs of northern gannets. *Journal of Experimental Biology* **217**, 876–885. (doi:10.1242/jeb.097915).

3. Hedenström, A. & Bone, Q., 1993 Migration by soaring or flapping flight in birds: the relative importance of energy cost and speed. *Philosophical Transactions of the Royal Society of London. Series B: Biological Sciences* **342**, 353–361. (doi:10.1098/rstb.1993.0164).

4. Sapir, N., Wikelski, M., McCue, M. D., Pinshow, B. & Nathan, R., 2010 Flight modes in migrating european bee-eaters: heart rate may indicate low metabolic rate during soaring and gliding. *PLoS One* **5**, e13956. (doi:10.1371/journal.pone.0013956).

5. Duriez, O., Kato, A., Tromp, C., Dell'Omo, G., Vyssotski, A. L., Sarrazin, F. & Ropert-Coudert, Y., 2014 How cheap is soaring flight in raptors? a preliminary investigation in freely-flying vultures. *PLoS One* **9**, e84887. (doi:10.1371/journal.pone.0084887).

6. Wilson, R. P., Quintana, F. & Hobson, V. J., 2012 Construction of energy landscapes can clarify the movement and distribution of foraging animals. *Proceedings of the Royal Society B: Biological Sciences* **279**, 975–980. (doi:10.1098/rspb.2011.1544).

7. Alerstam, T., 2001 Detours in bird migration. *Journal of Theoretical Biology* **209**, 319–331. (doi:10.1006/jtbi.2001.2266).

8. Bildstein, K. L., 2006 *Migrating raptors of the world: their ecology & conservation*. Cornell University Press.

9. Mellone, U., 2020 Sea crossing as a major determinant for the evolution of migratory strategies in soaring birds. *Journal of Animal Ecology* **89**, 1298–1301.

10. Zalles, J. I. & Bildstein, K. L., 2000 *Raptor watch a global directory of raptor migration sites*. 598.9 R221. Birdlife International, Cambridge, UK.

11. Newton, I., 2010 *The migration ecology of birds*. Elsevier.

12. Agostini, N., Malara, G., Neri, F., Mollicone, D. & Melotto, S., 1994 Flight strategies of honey buzzards during spring migration across the central mediterranean. *Avocetta* **18**, 73–76.

13. Agostini, N. & Duchi, A., 1994 Water-crossing behavior of black kites (milvus migrans) during migration. *Bird Behavior* **10**, 45–48.

14. Panuccio, M., Agostini, N. & Massa, B., 2002 Crossing the tyrrhenian sea: spring migration of marsh harriers (circus aeruginosus), sex classes and relation to wind conditions. *Vogelwarte* **41**, 271–274.

15. Meyer, S. K., Spaar, R. & Bruderer, B., 2000 To cross the sea or to follow the coast? flight directions and behaviour of migrating raptors approaching the mediterranean sea in autumn. *Behaviour* pp. 379–399.

16. Driscoll, P. V. & Ueta, M., 2002 The migration route and behaviour of eastern curlews numenius madagascariensis. *Ibis* **144**, E119–E130.

17. Gill Jr, R. E., Tibbitts, T. L., Douglas, D. C., Handel, C. M., Mulcahy, D. M., Gottschalck, J. C., Warnock, N., McCaffery, B. J., Battley, P. F. & Piersma, T., 2009 Extreme endurance flights by landbirds crossing the pacific ocean: ecological corridor rather than barrier? *Proceedings of the Royal Society B: Biological Sciences* **276**, 447–457.

18. Nourani, E., Yamaguchi, N. M., Manda, A. & Higuchi, H., 2016 Wind conditions facilitate the seasonal water-crossing behaviour of oriental honey-buzzards pernis ptilorhynchus over the east china sea. *Ibis* **158**, 506–518. (doi:10.1111/ibi.12383).

19. Nourani, E., Vansteelant, W. M., Byholm, P. & Safi, K., 2020 Dynamics of the energy seascape can explain intra-specific variations in sea-crossing behaviour of soaring birds. *Biology Letters* **16**, 20190797. (doi: doi.org/10.1098/rsbl.2019.0797).

20. Agostini, N., Panuccio, M. & Pasquaretta, C., 2015 Morphology, flight performance, and water crossing tendencies of afro-palearctic raptors during migration. *Current Zoology* **61**, 951–958.

21. Mitchell, G. W., Woodworth, B. K., Taylor, P. D. & Norris, D. R., 2015 Automated telemetry reveals age specific differences in flight duration and speed are driven by wind conditions in a migratory songbird. *Movement Ecology* **3**, 19. (doi:10.1186/s40462-015-0046-5).

22. Oppel, S., Dobrev, V., Arkumarev, V., Saravia, V., Bounas, A., Kret, E., Velevski, M., Stoychev, S. & Nikolov, S. C., 2015 High juvenile mortality during migration in a declining population of a long-distance migratory raptor. *Ibis* **157**, 545–557. (doi:10.1111/ibi.12258).

23. Nourani, E., Safi, K., Yamaguchi, N. M. & Higuchi, H., 2018 Raptor migration in an oceanic flyway: wind and geography shape the migratory route of grey-faced buzzards in east asia. *Royal Society open science* **5**, 171555. (doi:doi.org/10.1098/rsos.171555).

24. Becciu, P., Rotics, S., Horvitz, N., Kaatz, M., Fiedler, W., Zurell, D., Flack, A., Jeltsch, F., Wikelski, M., Nathan, R. *et al.*, 2020 Causes and consequences of facultative sea crossing in a soaring migrant. *Functional Ecology* **34**, 840–852. (doi:10.1111/1365-2435.13539).

25. Weimerskirch, H., Chastel, O., Barbraud, C. & Tostain, O., 2003 Frigatebirds ride high on thermals. *Nature* **421**, 333–334.

26. Yamaguchi, N. M., Arisawa, Y., Shimada, Y. & Higuchi, H., 2012 Real-time weather analysis reveals the adaptability of direct sea-crossing by raptors. *Journal of ethology* **30**, 1–10.

27. Duriez, O., Peron, G., Gremillet, D., Sforzi, A. & Monti, F., 2018 Migrating ospreys use thermal uplift over the open sea. *Biology letters* **14**, 20180687. (doi:10.1098/rsbl.2018.0687).

28. Woodcock, A. H., 1940 Convection and soaring over the open sea. *Journal of Marine Research* **3**, 248–253.

29. Stull, R. B., 2012 *An introduction to boundary layer meteorology*, volume 13. Springer Science & Business Media.

30. Vansteelant, W., Kekkonen, J. & Byholm, P., 2017 Wind conditions and geography shape the first outbound migration of juvenile honey buzzards and their distribution across sub-saharan africa. *Proceedings of the Royal Society B: Biological Sciences* **284**, 20170387. (doi:10.1098/rspb.2017.0387).

31. Yoda, K., Yamamoto, T., Suzuki, H., Matsumoto, S., Müller, M. & Yamamoto, M., 2017 Compass orientation drives naïve pelagic seabirds to cross mountain ranges. *Current Biology* **27**, R1152–R1153.

32. Dodge, S., Bohrer, G., Weinzierl, R., Davidson, S. C., Kays, R., Douglas, D., Cruz, S., Han, J., Brandes, D. & Wikelski, M., 2013 The environmental-data automated track annotation (env-data) system: linking animal tracks with environmental data. *Movement Ecology* **1**, 3. (doi:10.1186/2051-3933-1-3).

33. Bohrer, G., Brandes, D., Mandel, J. T., Bildstein, K. L., Miller, T. A., Lanzone, M., Katzner, T., Maisonneuve, C. & Tremblay, J. A., 2012 Estimating updraft velocity components over large spatial scales: contrasting migration strategies of golden eagles and turkey vultures. *Ecology letters* **15**, 96–103.

34. Dixon, A., Batbayar, N. & Purev-Ochir, G., 2011 Autumn migration of an amur falcon falco amurensis from mongolia to the indian ocean tracked by satellite. *Forktail* **27**, 81–84.

35. Meyburg, B., Meyburg, C. & Pretorius, R., 2017 Year-round satellite tracking of amur falcon (falco amurensis) reveals the longest migration of any raptor species across the open sea. In *From avian tracking to population processes, British Ornithologists' Union Annual Conference University of Warwick*.

36. Wood, S., 2019 Package ‘mgcv’. *R package version 1.8-31* .

37. R Core Team, 2020 *R: A Language and Environment for Statistical Computing*. R Foundation for Statistical Computing, Vienna, Austria.

38. Fortin, D., Beyer, H. L., Boyce, M. S., Smith, D. W., Duchesne, T. & Mao, J. S., 2005 Wolves influence elk movements: behavior shapes a trophic cascade in yellowstone national park. *Ecology* **86**, 1320–1330. (doi:10.1890/04-0953).

39. Kranstauber, B., Smolla, M. & Scharf, A. K., 2020 Package ‘move’ .

40. Safi, K., Kranstauber, B., Weinzierl, R., Griffin, L., Rees, E. C., Cabot, D., Cruz, S., Proaño, C., Takekawa, J. Y., Newman, S. H. *et al.*, 2013 Flying with the wind: scale dependency of speed and direction measurements in modelling wind support in avian flight. *Movement Ecology* **1**, 4. (doi:10.1186/2051-3933-1-4).

41. Lindgren, F., Rue, H. *et al.*, 2015 Bayesian spatial modelling with r-inla. *Journal of Statistical Software* **63**, 1–25. (doi:10.18637/jss.v063.i19).

42. Muff, S., Signer, J. & Fieberg, J., 2019 Accounting for individual-specific variation in habitat-selection studies: Efficient estimation of mixed-effects models using bayesian or frequentist computation. *Journal of Animal Ecology* **89**, 80–92. (doi:10.1111/1365-2656.13087).

43. Gómez-Rubio, V., 2020 *Bayesian inference with INLA*. CRC Press.

44. Schmaljohann, H. & Naef-Daenzer, B., 2011 Body condition and wind support initiate the shift of migratory direction and timing of nocturnal departure in a songbird. *Journal of Animal Ecology* **80**, 1115–1122.

45. Gill Jr, R. E., Douglas, D. C., Handel, C. M., Tibbitts, T. L., Hufford, G. & Piersma, T., 2014 Hemispheric-scale wind selection facilitates bar-tailed godwit circum-migration of the pacific. *Animal Behaviour* **90**, 117–130.

46. Bradarić, M., Bouten, W., Fijn, R. C., Krijgsveld, K. L. & Shamoun-Baranes, J., 2020 Winds at departure shape seasonal patterns of nocturnal bird migration over the north sea. *Journal of Avian Biology* **51**.

47. Agostini, N., Lucia, G., Mellone, U., Panuccio, M., Von Hardenberg, J., Evangelidis, A. & Kominos, T., 2012 Loop migration of adult european honey buzzards (pernis apivorus linnaeus, 1758) through the central-eastern mediterranean. *Italian Journal of Zoology* **79**, 280–286.

48. Kranstauber, B., Weinzierl, R., Wikelski, M. & Safi, K., 2015 Global aerial flyways allow efficient travelling. *Ecology letters* **18**, 1338–1345. (doi:10.1111/ele.12528).

49. Panuccio, M., Barboutis, C., Chiatante, G., Evangelidis, A. & Agostini, N., 2016 Pushed by increasing air temperature and tailwind speed: weather selectivity of raptors migrating across the aegean sea. *Ornis Fennica* **93**, 159–172.

50. Nourani, E., Yamaguchi, N. M. & Higuchi, H., 2017 Climate change alters the optimal wind-dependent flight routes of an avian migrant. *Proceedings of the Royal Society B: Biological Sciences* **284**, 20170149. (doi:10.1098/rspb.2017.0149).

51. Santos, C. D., Silva, J. P., Muñoz, A.-R., Onrubia, A. & Wikelski, M., 2020 The gateway to africa: what determines sea crossing performance of a migratory soaring bird at the strait of gibraltar? *Journal of Animal Ecology* **89**, 1317–1328. (doi:10.1111/1365-2656.13201).

52. Woodcock, A. H., 1975 Thermals over the sea and gull flight behavior. *Boundary-Layer Meteorology* **9**, 63–68.

53. Fortin, D., Liechti, F. & Brudere, B., 1999 Variation in the nocturnal flight behaviour of migratory birds along the northwest coast of the mediterranean sea. *Ibis* **141**, 480–488. (doi:10.1111/j.1474-919X.1999.tb04417.x).

54. Norevik, G., Åkesson, S., Artois, T., Beenaerts, N., Conway, G., Cresswell, B., Evens, R., Henderson, I., Jiguet, F. & Hedenström, A., 2020 Wind-associated detours promote seasonal migratory connectivity in a flapping flying long-distance avian migrant. *Journal of Animal Ecology* **89**, 635–646. (doi:10.1111/1365-2656.13112).

55. La Sorte, F. A., Fink, D., Hochachka, W. M. & Kelling, S., 2016 Convergence of broad-scale migration strategies in terrestrial birds. *Proceedings of the Royal Society B: Biological Sciences* **283**, 20152588. (doi:10.1098/rspb.2015.2588).

56. Cano, N., Bayly, N. J. & Wilson, S., 2020 Is there more than one way to cross the caribbean sea? migratory strategies of nearctic-neotropical landbirds departing from northern colombia. *Journal of Avian Biology* **51**. (doi:10.1111/jav.02394).

57. Bowlin, M. S. & Wikelski, M., 2008 Pointed wings, low wingloading and calm air reduce migratory flight costs in songbirds. *PloS one* **3**, e2154.

58. Anderson, R. C., 2009 Do dragonflies migrate across the western indian ocean? *Journal of Tropical Ecology* **25**, 347–358. (doi:10.1017/S0266467409006087).

59. Davaasuren, B., Erdenechimeg, T. & Sukhbaatar, T., 2019 *Mongolian Bird Ringing Program: Annual Report 2019*. Wildlife Science and Conservation Center of Mongolia.

Supplementary material

Supplementary Figure 1

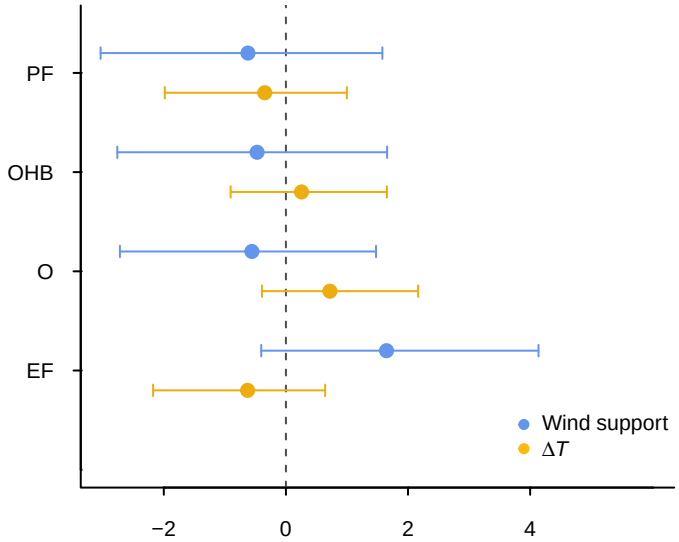

Figure S1: Species-specific variation in route selection. Posterior means and 95 % credible intervals are shown for the species-level random effects of the best INLA model (Model 3 in Table 1).

Supplementary Figure 2

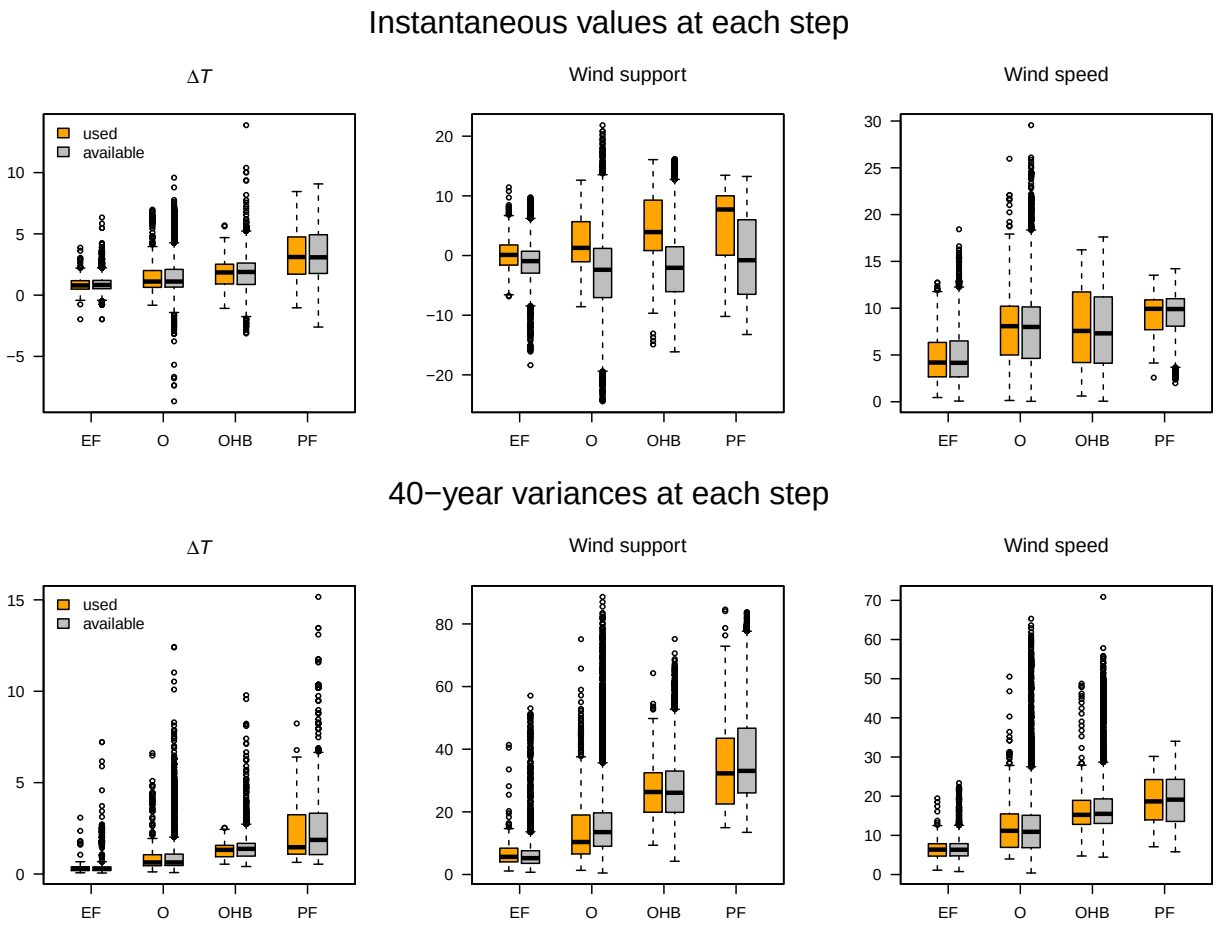

Figure S2: Distribution of values over the used and available steps. These were used for building the step-selection functions. The top row shows the instantaneous values and the bottom row the long-term variances. In the top row, it can be seen that wind support has more variability than ΔT and higher values of wind support are selected by the birds.

496 Supplementary Figure 3

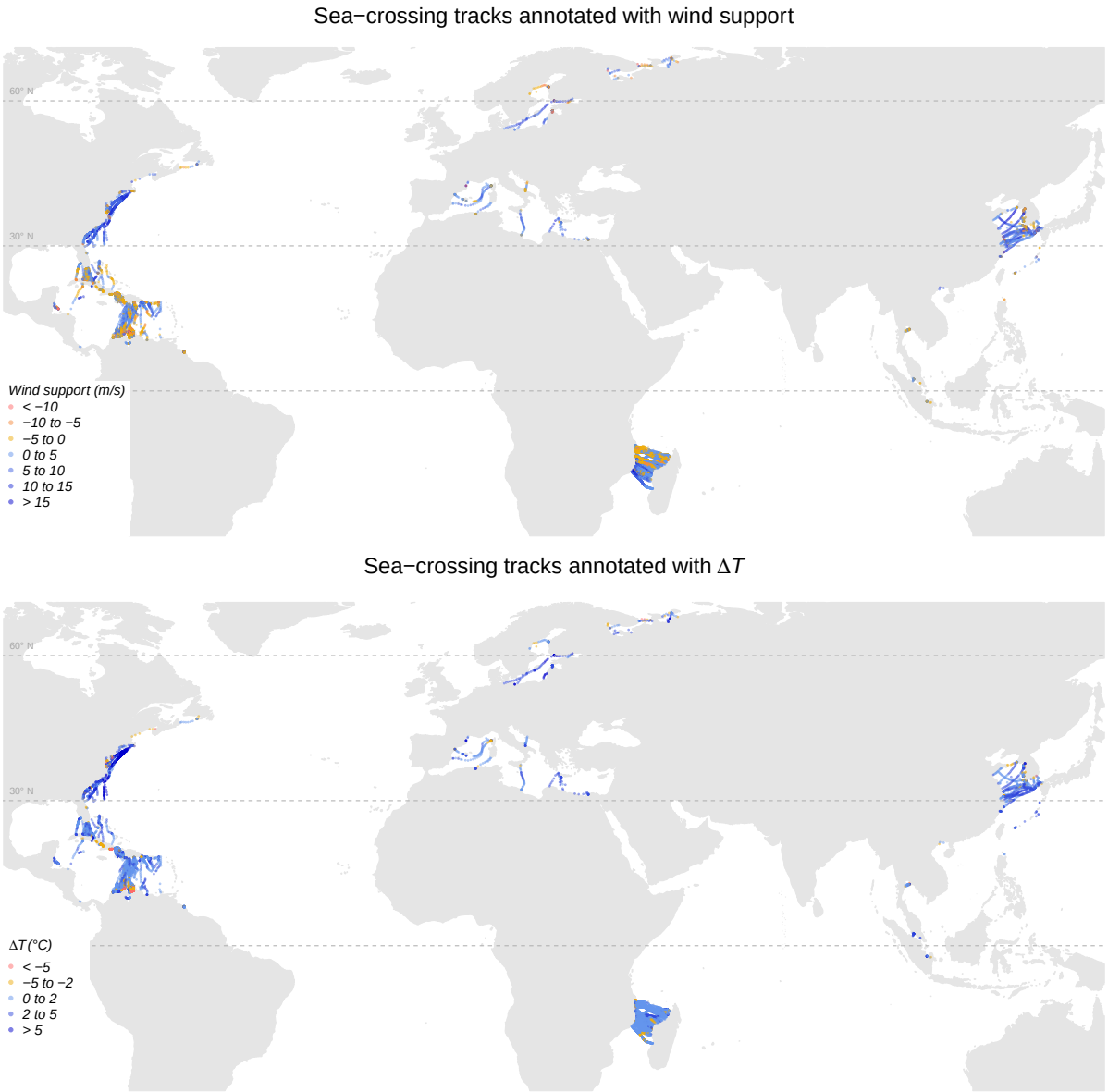

Figure S3: Bio-logging data for sea-crossing tracks annotated with wind support and ΔT. Data is pooled for sea-crossing segments during autumn migration of the Oriental honey buzzard *Pernis ptilorhynchus* and the grey-faced buzzard *Butastur indicus* in the East Asian flyways, the osprey *Pandion haliaetus* and the peregrine falcon *Falco peregrinus*, in both the African-Eurasian and the American flyways, and the Eleonora's falcon *Falco eleonorae* in the African-Eurasian flyway. For samples of complete tracks, see Fig. 2.

Supplementary Figure 4

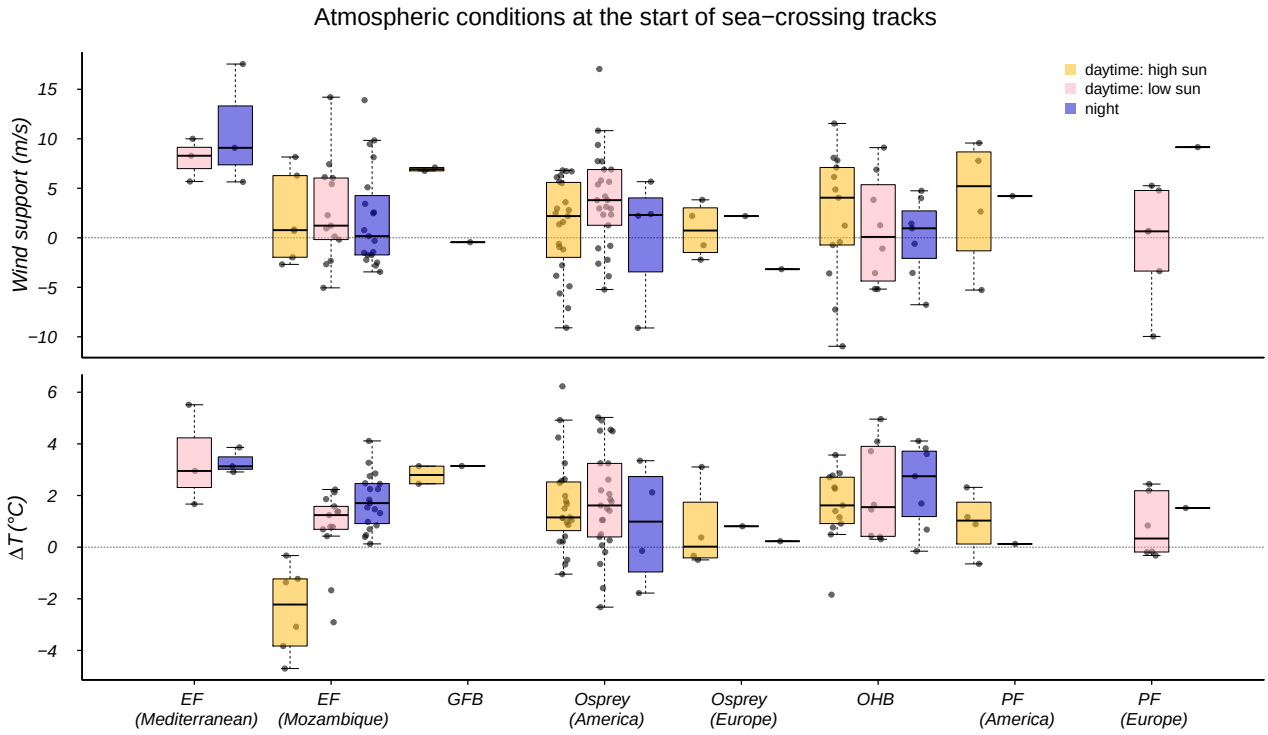

Figure S4: Wind support and ΔT values at the start of each sea-crossing track, grouped by time of day. Most species initiated sea-crossing with positive ΔT and tailwind. An overview of wind support and ΔT along the sea-crossing tracks is presented in Fig. S3.

Supplementary Table 1

Table S1: Summary of bio-logging data used in the step-selection function analysis. The number of individuals and migratory tracks correspond to the data that were retained after filtering the raw data set (see methods). The corresponding Movebank study names are shown in the footnotes.

Species	Tagging_location	Device	Years	Individuals	Tracks
Eleonora's falcon	Greece	GPS	2015	3	3
Eleonora's falcon	Spain	GPS	2012-2018	10	19
Oriental honey buzzard	Japan	GPS	2017-2019	8	17
Osprey [a]	South Europe	GPS	2013-2019	4	4
Osprey [b]	North America	GPS	2010-2019	10	15
Peregrine falcon [c]	North Europe	GPS	2018-2020	4	5
Peregrine falcon [c]	North America	GPS	2016	3	3
Totals				42	66

[a] Osprey in Mediterranean (Corsica, Italy, Balearics)

[b] Osprey Bierregaard North and South America

[c] LifeTrack Peregrine falcon

Supplementary Table 2

Table S2: Results of regional GAMMs built using forty years of global temperature data. These models were used for constructing energy seascapes (Fig. 2).

East Asia

A. parametric coefficients	Estimate	Std. Error	t-value	p-value
(Intercept)	-0.5051	0.0092	-54.9250	< 0.0001
sun_elev_flow	2.1566	0.0114	189.5042	< 0.0001
sun_elev_fnight	2.3400	0.0103	227.6074	< 0.0001
B. smooth terms	edf	Ref.df	F-value	p-value
s(lat,lon):sun_elev_fhigh	88.4643	88.4643	97.8487	< 0.0001
s(lat,lon):sun_elev_flow	91.2851	91.2851	196.2278	< 0.0001
s(lat,lon):sun_elev_fnight	92.7295	92.7295	190.2838	< 0.0001
s(yday):sun_elev_fhigh	7.6664	8.0000	231.6346	< 0.0001
s(yday):sun_elev_flow	7.7456	8.0000	228.6311	< 0.0001
s(yday):sun_elev_fnight	7.7940	8.0000	471.8103	< 0.0001
s(year)	0.0000	1.0000	0.0018	< 0.0001

The Americas

A. parametric coefficients	Estimate	Std. Error	t-value	p-value
(Intercept)	0.0296	0.0108	2.7394	0.0062
sun_elev_flow	1.3794	0.0129	106.6076	< 0.0001
sun_elev_fnight	1.6410	0.0126	130.5864	< 0.0001
B. smooth terms	edf	Ref.df	F-value	p-value
s(lat,lon):sun_elev_fhigh	90.0437	90.0437	169.5629	< 0.0001
s(lat,lon):sun_elev_flow	94.5179	94.5179	141.5539	< 0.0001
s(lat,lon):sun_elev_fnight	95.7668	95.7668	197.9859	< 0.0001
s(yday):sun_elev_fhigh	7.4179	8.0000	326.2731	< 0.0001
s(yday):sun_elev_flow	7.4498	8.0000	787.2890	< 0.0001
s(yday):sun_elev_fnight	7.2856	8.0000	524.7097	< 0.0001
s(year)	0.0000	1.0000	0.0000	0.8275

Indian Ocean

A. parametric coefficients	Estimate	Std. Error	t-value	p-value
(Intercept)	-0.1858	0.0051	-36.2476	< 0.0001
sun_elev_flow	0.0578	0.0065	8.8270	< 0.0001
sun_elev_fnight	1.2402	0.0057	216.8062	< 0.0001
B. smooth terms	edf	Ref.df	F-value	p-value
s(lat,lon):sun_elev_fhigh	94.7248	94.7248	231.4795	< 0.0001
s(lat,lon):sun_elev_flow	96.0323	96.0323	170.5800	< 0.0001
s(lat,lon):sun_elev_fnight	95.7945	95.7945	151.6102	< 0.0001
s(yday):sun_elev_fhigh	7.9279	8.0000	1455.4752	< 0.0001
s(yday):sun_elev_flow	7.9261	8.0000	1537.6625	< 0.0001
s(yday):sun_elev_fnight	7.9736	8.0000	5190.4193	< 0.0001
s(year)	0.0000	1.0000	0.0000	0.8801

Europe

A. parametric coefficients	Estimate	Std. Error	t-value	p-value
(Intercept)	-1.3977	0.0943	-14.8277	< 0.0001
sun_elev_flow	2.3936	0.0953	25.1193	< 0.0001
sun_elev_fnight	3.4697	0.0955	36.3168	< 0.0001
B. smooth terms	edf	Ref.df	F-value	p-value
s(lat,lon):sun_elev_fhigh	2.0000	2.0000	56.3685	< 0.0001
s(lat,lon):sun_elev_flow	75.6502	75.6502	14.5510	< 0.0001
s(lat,lon):sun_elev_fnight	82.6352	82.6352	40.0598	< 0.0001
s(yday):sun_elev_fhigh	6.0995	8.0000	210.8682	< 0.0001
s(yday):sun_elev_flow	7.8303	8.0000	1434.8943	< 0.0001
s(yday):sun_elev_fnight	7.6710	8.0000	1046.5831	< 0.0001
s(year)	0.0000	1.0000	0.0000	0.0634

Mozambique Channel

A. parametric coefficients	Estimate	Std. Error	t-value	p-value
(Intercept)	0.1469	0.0279	5.2605	< 0.0001
sun_elev_flow	0.2450	0.0334	7.3248	< 0.0001
sun_elev_fnight	1.7059	0.0280	61.0334	< 0.0001
B. smooth terms	**edf**	**Ref.df**	**F-value**	**p-value**
s(lat,lon):sun_elev_fhigh	89.1660	89.1660	30.6120	< 0.0001
s(lat,lon):sun_elev_flow	71.4595	71.4595	165.7619	< 0.0001
s(lat,lon):sun_elev_fnight	95.5807	95.5807	83.2314	< 0.0001
s(yday):sun_elev_fhigh	6.5492	8.0000	362.2948	< 0.0001
s(yday):sun_elev_flow	7.5523	8.0000	299.7936	< 0.0001
s(yday):sun_elev_fnight	7.5972	8.0000	608.8270	< 0.0001
s(year)	0.0001	1.0000	0.0002	0.0780